Myers K.J., Reeder M.F., Bakker A., Dickey D.S. (1997) A Parametric Study of the Performance of the Prochem Maxflo T Impeller. Recents Progres en Genie des Procedes, Vol. 11, No. 52, page 115-122.

Récents Progres en Génie des Procédés
Volume 11, number 52 (1997), pp. 115 - 122
ISBN 2-910239-26-8
ed. Lavoisier, Paris, France

A PARAMETRIC STUDY OF THE PERFORMANCE OF THE PROCHEM MAXFLO T IMPELLER

MYERS K.[1], REEDER M.F.[2], BAKKER A.[2], DICKEY D.S.[2]

◊ (1) CHEMICAL & MATERIALS ENGINEERING
Univ. of Dayton
DAYTON, Ohio 45469-0246, USA

◊ (2) CHEMINEER, Inc.
PO BOX 1123
DAYTON, Ohio 45401-1123, USA

Abstract. The effects of blade number and blade tip angle on the performance of the Maxflo T impeller have been studied. Specifically, the laminar, transitional, and turbulent power draw, gassed power draw in mixed impeller systems, and solids suspension performance of the Maxflo T have been characterized. In general, the Maxflo T outperforms the pitched-blade turbine and can be used in applications where low power number high-efficiency impellers are impractical because of shaft critical speed and/or diameter limitations.

Résumé. La performance de l´agitateur Maxflo T a été mise en évidence grâce aux effets du nombre de lames et leur bout angulaire. Précisément, la puissance laminaire, transitoire, et turbulente, la puissance gazeuse consommée dans les systèmes des agitateurs mixtes et la performance en suspension des solides du Maxflo T on été caractérisées. En général, la performance du Maxflo T est meilleure que celle de la turbine a lame inclinée. Le Maxflo T peut être utilisé dans les applications dont lesquelles les agitateurs de haute efficacité ayant un degré de puissance inférieur ne sont pas pratiques et cela est dû a la fréquence critique de la tige et/ou alors aux limitations des grades diamètres.

The Maxflo T impeller is a high-solidity, axial-flow impeller that provides superior performance in a wide range of applications including liquid blending, solids suspension, and gas dispersion. This impeller performs particularly well in fermentation processes, with numerous studies reported in the literature, including Gbewonyo et al. (1986) and Buckland et al. (1988). Most of these studies have not considered the geometric versatility of this impeller. In particular, the three, four, five and six-blade versions of the Maxflo T provide design flexibility. Further, the blade tip angle can be adjusted to optimize performance for a particular application. This study examined the influence of these impeller design variables on the laminar, transitional, and turbulent power draw, gassed power draw in mixed impeller systems, and solids suspension performance of the Maxflo T. A four-bladed version of the Maxflo T impeller is shown in Figure 1. A Chemineer HE-3 impeller is also included in this figure as an example of a low-solidity, low power number high-efficiency impeller.

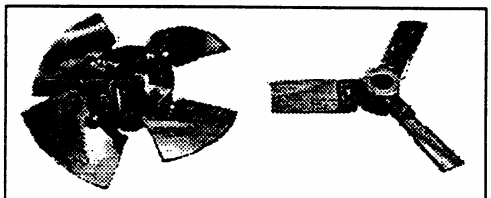

Figure 1: The Prochem Maxflo T (left) and Chemineer HE-3 (right) Impellers

EXPERIMENTAL APPARATUS AND PROCEDURE

The time-averaged turbulent velocity field of the Maxflo T was determined in water using digital particle image velocimetry (DPIV) in a flat-bottomed cylindrical vessel. Willert and Gharib (1991) have described the DPIV technique in detail, while Myers et al. (1996a) have discussed its application in agitated systems. The impeller diameter was 0.127 m and the vessel diameter was 0.292 m (D/T =

0.435). Square-batch geometry (Z/T = 1) and an off-bottom clearance of one-third of the tank diameter (C/T = 0.333) were used.

Turbulent, single-phase power draw data were taken in water under the following conditions (unless noted as different): N_b = 3, 4, and 6, D = 0.104, 0.151, and 0.230 m, various T such that $0.11 \leq D/T \leq 0.67$, C/T = 0.333, Z/T = 1, and β = 18° to 26° in 2° increments. All vessels were flat-bottomed with four standard vertical baffles (width equal to T/12, offset from the vessel wall by a distance of T/72). Torque was measured with calibrated reaction strain gauges and speed was measured with a zero velocity magnetic pickup.

Transitional and laminar regime power draws were taken in aqueous glycerine and corn syrup solutions with limited variation of parameters (N_b = 3 and 6, β = 20° and 30°, D = 0.140 m, T = 0.341 m, D/T = 0.411, C/T = 0.333, and Z/T = 1).

Dual mixed CD-6/Maxflo T impeller systems were studied in air-water dispersions in a 0.394 m, dish-bottomed vessel. The CD-6 is a six-bladed, disc turbine with semicircular blades that has gas dispersion characteristics that are superior to those of the Rushton turbine. The pertinent geometric parameters for this study were: D_{CD-6}/T = 0.41, D_{MFT}/T = 0.58, C_{CD-6}/T = 0.25, S = T/2, Z_o/T = 1.2, and β = 18°. The Maxflo T was always used in the down-pumping mode, and gas was introduced through a 0.102 m ring sparger centered below the CD-6 impeller. Froude numbers ($N_{Fr} = N^2D/g$) of 0.3, 0.6, and 0.9 based on the CD-6 diameter were considered.

The gassed power draw of the Maxflo T was measured using a large ring sparger to simulate the environment that the Maxflo T experiences as an upper, pumping impeller in mixed impeller systems. The experimental system was basically the same used to study the mixed CD-6/Maxflo T impeller systems with the following differences: D/T = 0.48 and 0.58, β: 18°, 22°, and 26°, S = T/2 and T, and sparge ring diameter = 0.279 m.

Physical property effects in solids suspension were studied under the following conditions: flat-bottomed vessel, T = 0.292 m, D/T = 0.35, C/T = 0.25, Z/T = 1, X = 0.05, N_b = 3, 4, and 6, and β = 19.3°, 22.5°, and 25.5°. All solids suspension experiments were performed in water with solids that spanned the range of pertinent physical properties. The performance of the Maxflo T was compared to a pitched-blade turbine (termed the P-4, with N_b = 4, β = 45°, and W/D = 0.20) and a high-efficiency impeller (the Chemineer HE-3 of standard construction). These impellers were studied at the same conditions as the Maxflo T (i.e.: X = 0.05, D/T = 0.35, C/T = 0.25, etc.).

Two vessels (T = 0.343 and 0.597 m) were used to study the influence of impeller diameter to tank diameter ratio (D/T) on the just-suspended speed over a broad range of this parameter ($0.11 \leq D/T \leq 0.67$). To compare data taken on two different scales, a relative just-suspended speed, $N_{js}(D/T)/N_{js}(D/T = 0.35)$ was used. The geometries that lead to flow reversal were determined in the 0.343 m vessel at a solids loading of five weight percent (X = 0.05). Flow reversal occurs when the impeller discharge flow impinges on the vessel wall rather than the base. This condition leads to radially-inward flow across the vessel base and high just-suspended speed, torque, and power requirements.

RESULTS AND DISCUSSION

Velocity Field

The time-averaged turbulent velocity field of the Maxflo T is shown in Figure 2 (N_b = 4, β = 18°, D/T = 0.435, C/T = 0.333, and Z/T = 1). This velocity field, determined using DPIV, clearly illustrates the highly axial flow field produced by the Maxflo T impeller. The flow field is slightly asymmetric because the plane of study was 0.01 m in front of a plane defined by two baffles and the shaft. When viewed from above, the impeller was rotating clockwise. Thus, the right side of the flow field is just behind a baffle and the left side of the flow field is just in front of a baffle.

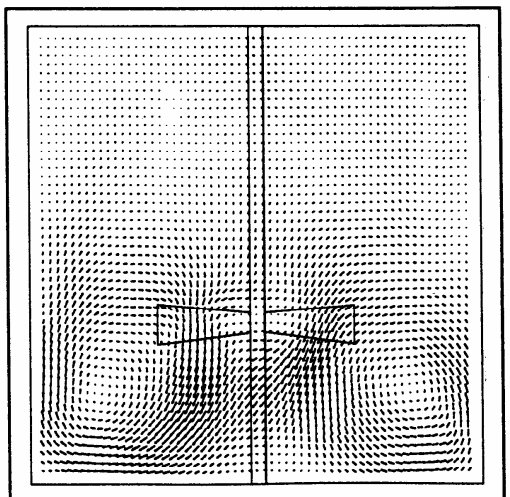

Figure 2: The time-averaged turbulent velocity field of the Maxflo T impeller

Power Draw

Figure 3 demonstrates the influence of blade tip angle and impeller diameter to tank

diameter ratio (D/T) on the turbulent power number of the three-bladed Maxflo T impeller (C/T = 0.333 and Z/T = 1). The power number decreases slowly as the impeller diameter to tank diameter ratio increases from eleven to fifty-two percent ($0.11 \leq D/T \leq 0.52$). This behavior is typical of axial-flow impellers (Fasano et al.,1994). For larger impeller diameter to tank diameter ratios ($0.52 \leq D/T \leq 0.67$), the power number increases dramatically. This increase is caused by a change in the flow pattern from the impeller discharge flow impinging on the vessel base to the discharge flow impinging on the vessel wall. This flow pattern change will also be shown to influence solids suspension performance.

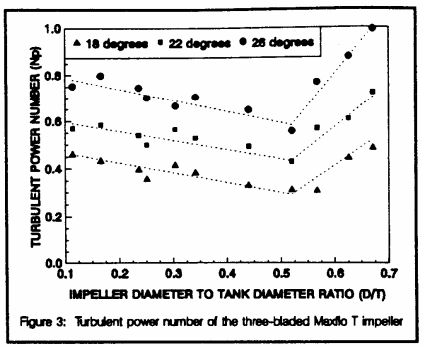

Figure 3: Turbulent power number of the three-bladed Maxflo T impeller

The expected increase in turbulent power number with increasing blade tip angle can be seen in Figure 3. This effect is further examined in Figure 4 which shows that the turbulent power number increases in a nearly linear manner with increasing blade tip angle ($N_b = 3$, C/T = 0.333, and Z/T = 1).

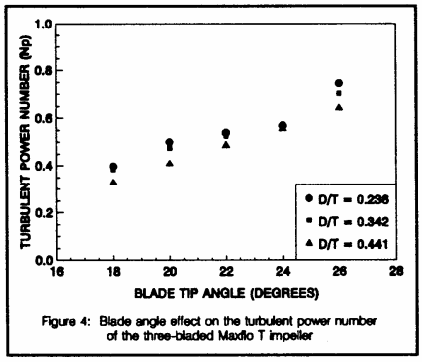

Figure 4: Blade angle effect on the turbulent power number of the three-bladed Maxflo T impeller

Additional blades increase the turbulent power number of the Maxflo T impeller as shown in Figure 5 (C/T = 0.333, Z/T = 1, and $\beta = 22°$). The following equations relate the turbulent power number of the Maxflo T to the number of blades.

$$N_p(N_b=6)=1.09\,N_p(N_b=5)=$$

$$1.20N_p(N_b=4)=1.37N_p(N_b=3) \quad (1)$$

Note that the five-bladed Maxflo T was not studied; rather, interpolation was used to infer its turbulent power number. These relations can be generalized as

$$N_p \propto N_b^{0.45} \quad (2)$$

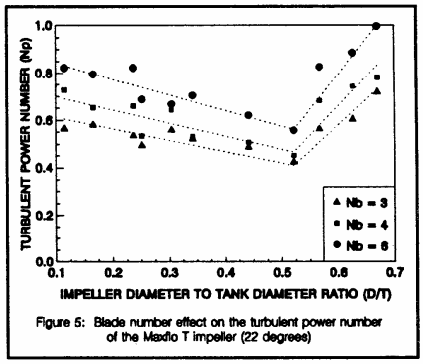

Figure 5: Blade number effect on the turbulent power number of the Maxflo T impeller (22 degrees)

Limited data was taken concerning the effect of off-bottom clearance on the turbulent power number of the Maxflo T ($N_b = 3$, $0.17 \leq D/T \leq 0.52$, and $\beta = 22°$). For intermediate clearances ($0.25 \leq C/T \leq 0.45$) the power number was essentially constant. Higher power numbers (as much as forty percent higher) were observed at lower and higher clearances. The increases in turbulent power numbers were greater for larger impeller diameter to tank diameter ratios.

The effect of impeller Reynolds number on the Maxflo T power number is shown in Figure 6 (on the following page; $N_b = 3$ and 6, $\beta = 20°$ and 30°, D = 0.140 m, T = 0.341 m, D/T = 0.411, C/T = 0.333, and Z/T = 1). At Reynolds numbers less than 10, laminar operation is observed, with the power number being inversely proportional to the Reynolds number. In this regime, with viscous effects dominating the power draw, blade angle no longer influences the power number. The influence of the number of blades on the power number is slightly larger in the laminar regime than in the turbulent regime ($N_p(N_b=6) = 1.46\ N_p(N_b=3)$ in laminar operation, while the multiplier was found to be 1.37 in turbulent operation).

Gassed Power Draw

High solidity axial-flow impellers have been found to perform well in gas dispersion operations due to their ability to provide good top-to-bottom mixing in multiple impeller systems (Gbewonyo et al., 1986, and Buckland et al., 1988). However, when used to disperse gas, axial-flow impellers can exhibit substantial torque fluctuations (McFarlane and Nienow, 1995). This behavior has led to the use of mixed

impeller systems in which the incoming gas is dispersed by a lower, radial-flow turbine while upper axial-flow impellers provide top-to-bottom blending. These mixed impeller systems ensure good mixing performance while avoiding torque instabilities (Bakker et al., 1994a, and Myers et al., 1994)).

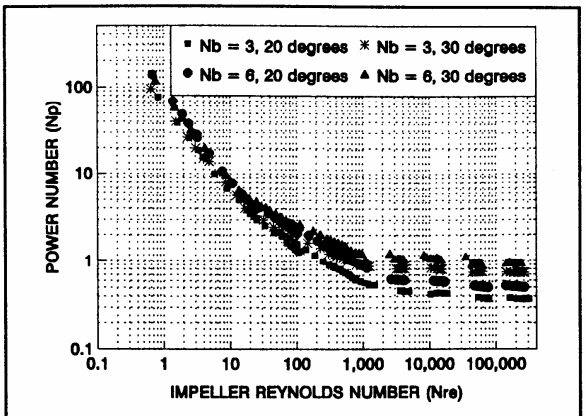

Figure 6: Reynolds number effect on the Maxflo T impeller power number

Because of their importance to process performance and typically large size (and associated capital investment), accurate prediction of the gassed power draw of multiple impeller systems is critical. Russell (1995) studied gassed power draw of mixed impeller systems (CD-6/HE-3) and found that their gassed power draw could be accurately predicted from the gassed power draw of the individual impellers in the following manner (M, D, and P refer to the mixed impeller system, the lower radial-flow dispersing impeller, and the upper axial-flow pumping impeller(s), respectively).

$$\left(\frac{P_g}{P_o}\right)_M = \alpha\left(\frac{P_g}{P_o}\right)_D + (1 - \alpha)\left(\frac{P_g}{P_o}\right)_P \qquad (3)$$

The gassed power draw of the individual impellers should be determined at the operating conditions of the mixed impeller system (i.e. - at the same gassing rate and speed of agitation). α is not an adjustable parameter used to fit data; rather, it is calculated *a priori* from the ungassed power draw of the individual impellers.

$$\alpha = \frac{N_{p_D} D_D^5}{N_{p_D} D_D^5 + n_P N_{p_P} D_P^5} \qquad (4)$$

n_P is the number of upper, pumping impellers in the system. The success of this approach relies on measuring the gassed power draws of the individual impellers under the appropriate conditions. Russell (1995) found that the gassed power draw of the dispersing impeller should be determined using the actual sparger configuration that is to be used in the mixed impeller system, but without any upper, axial-flow impellers present. Various techniques have been used to simulate the environment of the upper pumping impellers in mixed impeller systems, with the most common being a sheet sparger that distributes the gas uniformly over the vessel cross section, much like the lower dispersing impeller. For the mixed CD-6/Maxflo T impeller system it was found that a large ring sparger (significantly larger than the diameter of the pumping impeller) should be used to determine the gassed power draw of the Maxflo T. Figure 7 compares the gassed power draw predictions of a dual (n_P = 1) CD-6/Maxflo T system with experimental data, and the agreement can be seen to be good ($D_{CD\text{-}6}$ = 0.160 m, D_{MFT} = 0.230 m, T = 0.394 m, N_b = 3, β = 18°, and N_{Fr} = 0.6; N_{Fr} = 0.3 and 0.9 yielded similar results; N_{Fr} and N_A are based on the CD-6 diameter). This agreement indicates that the gassed power draw of mixed impeller systems can be predicted given the gassed power draws of the individual impellers in the appropriate environment.

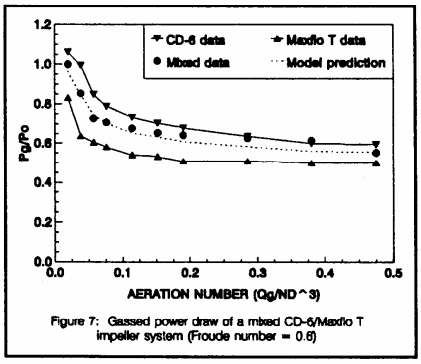

Figure 7: Gassed power draw of a mixed CD-6/Maxflo T impeller system (Froude number = 0.6)

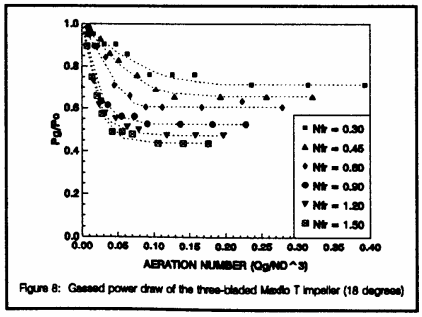

Figure 8: Gassed power draw of the three-bladed Maxflo T impeller (18 degrees)

The number of blades of the Maxflo T (N_b = 3, 4, or 6), the Maxflo T impeller diameter to tank diameter ratio (D/T = 0.48 or 0.58), and the separation between the CD-6 and Maxflo T (either T/2 or T) had minimal influence on the gassed power draw of the Maxflo T. Figure 8 (on the previous page) elucidates the dependence of the gassed power draw of the Maxflo T on the Froude and aeration numbers (N_b = 3, D/T = 0.48, S = T/2, and β = 18°; N_{Fr} and N_A now based on the Maxflo T diameter). The relative gassed power draw decreases with increasing Froude and aeration numbers (although at high aeration numbers the relative gassed power draw reaches a constant, asymptotic value). In Figure 9 the relative gassed power draw of the Maxflo T shows a decrease with increasing blade tip angle (N_b = 3, D/T = 0.58, S = T/2, and N_{Fr} = 0.6, with similar results found for N_b = 4 and 6). This decrease in gassed power draw of the Maxflo T with increasing blade angle can be described by the following relation.

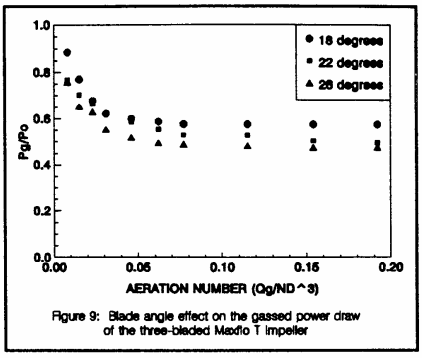

Figure 9: Blade angle effect on the gassed power draw of the three-bladed Maxflo T impeller

$$\frac{P_g}{P_o} \propto \beta^{-0.5} \qquad (5)$$

Solids Suspension

Corpstein et al. (1994) suggested that the just-suspended speed can be correlated with the adjusted settling velocity, u_a, which they defined as follows.

$$u_a = \left(\frac{\rho_s - \rho_l}{\rho_l}\right) u_t \qquad (6)$$

ρ_s and ρ_l represent the solid and liquid densities, respectively, and u_t represents the terminal settling velocity of the solid in quiescent liquid. The specific correlation was

$$N_{js} = k\, u_a^{0.28} \qquad (7)$$

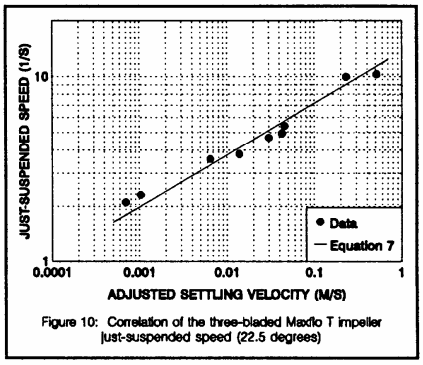

Figure 10: Correlation of the three-bladed Maxflo T impeller just-suspended speed (22.5 degrees)

where the coefficient k is a function of impeller type, solids loading, and system geometry (D/T, C/T, etc.). As shown in Figure 10, the just-suspended speed of the Maxflo T impeller can be described by this correlation. The data of Figure 10 were taken with N_b = 3, D/T = 0.35, C/T = 0.25, Z/T = 1, and X = 0.05. The just-suspended speeds of all versions of the Maxflo T that were studied could be correlated in the same manner, with the coefficient k being a function of the blade tip angle and number of blades.

The data of Figure 11 indicate that the just-suspended speed of the Maxflo T is intermediate between those of the pitched-blade turbine (P-4) and high-efficiency impeller (HE-3) (the P-4 turbine has been chosen as a reference impeller, and all other data is plotted relative to this reference; all impellers were studied at the same conditions of solids loading and geometry). The Maxflo T just-suspended speed is not significantly affected by the number of blades; the just-suspended speed of the four-bladed version is the same as that of the three-bladed version while the just-suspended speed of the six-bladed version is only four percent lower. However, the just-suspended speed of the Maxflo T does decrease with increasing blade tip angle.

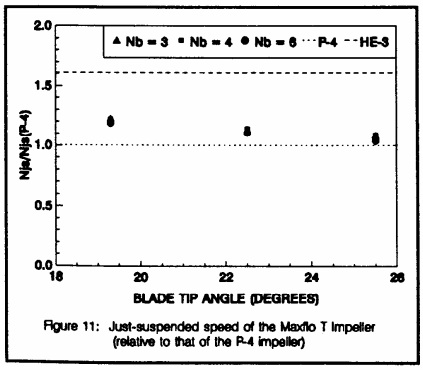

Figure 11: Just-suspended speed of the Maxflo T impeller (relative to that of the P-4 impeller)

$$N_{js} \propto \beta^{-0.45} \qquad (8)$$

The corresponding just-suspended torque and power requirements of the Maxflo T are presented in Figures 12 and 13 (again, relative to those of the P-4 turbine). The just-suspended torque requirements of the Maxflo T are always greater than the high-efficiency impeller (HE-3), but less than the pitched-blade turbine (P-4). The Maxflo T just-suspended torque always increases with increasing blade tip angle or increasing number of blades. The just-suspended power requirements of the Maxflo T are always less than the pitched-blade turbine and are often less than the high-efficiency impeller. The Maxflo T just-suspended power always increases with increasing blade number, but can be seen to increase (N_b = 3), remain constant (N_b = 4), or decrease (N_b = 6) with increasing blade tip angle.

The data of Figures 11 through 13 indicate that the solids suspension performance of the Maxflo T impeller generally deteriorates with increasing number of blades and increasing blade tip angle. Since the three-bladed Maxflo T has a higher power number than the high-efficiency impeller (HE-3), it does have a lower just-suspended speed. This suggests that the Maxflo T could be used in solids suspension applications where the higher speeds of the high-efficiency impeller are not practical because of critical shaft speed limitations. Use of the Maxflo T rather than the high-efficiency impeller leads to a higher torque requirement (but lower than that of the pitched-blade turbine (P-4)) and comparable power requirements.

The influence of impeller diameter to tank diameter ratio (D/T) on the just-suspended speed of the three-bladed Maxflo T is shown in Figure 14. The behavior of the Maxflo T is the same for both blade tip angles studied (β = 20° and 30°) and is very similar to the behavior of the high-efficiency impeller (HE-3) as discussed by Corpstein et al. (1994). Using the power number data presented previously, the just-suspended speed data can be used to calculate the corresponding just-suspended torque and power requirements of Figure 15 (note the power number data was taken at a higher clearance (C/T = 0.333) than the just-suspended speed data (C/T = 0.25), but the difference was considered to be negligible; also, the power number was taken to be constant for impeller diameter to tank diameter ratios greater than fifty-two percent because flow reversal occurs at a larger impeller diameter to tank diameter ratio at the lower off-bottom clearance of the solids suspension study).

The conclusions reached here for the just-suspended torque and power requirements are similar to those reported for the high-efficiency impeller (HE-3) studied by Corpstein et al. (1994). The just-suspended torque requirement increases continually with increasing impeller diameter to tank diameter ratio, with the rate of increase being dramatic for impeller diameter to tank diameter ratios greater than fifty-five percent (D/T > 0.55). The just-suspended power requirement decreases with increasing impeller diameter to tank diameter ratio at low impeller diameter to tank diameter ratios (D/T < 0.25).

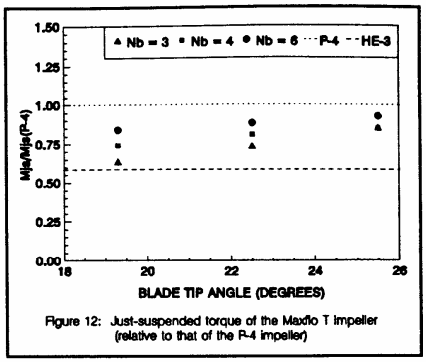

Figure 12: Just-suspended torque of the Maxflo T impeller (relative to that of the P-4 impeller)

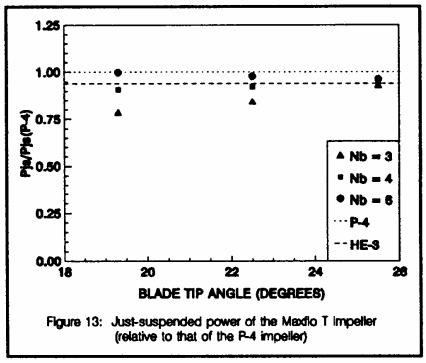

Figure 13: Just-suspended power of the Maxflo T impeller (relative to that of the P-4 impeller)

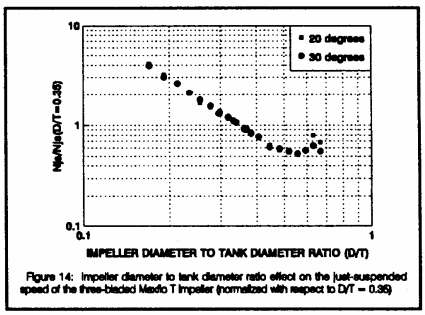

Figure 14: Impeller diameter to tank diameter ratio effect on the just-suspended speed of the three-bladed Maxflo T impeller (normalized with respect to D/T = 0.35)

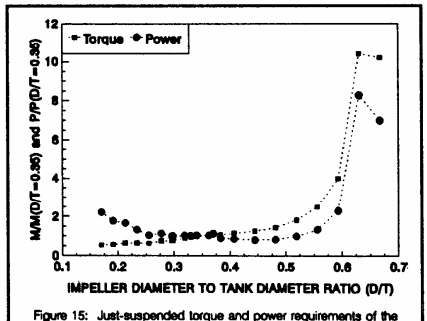

Figure 15: Just-suspended torque and power requirements of the three-bladed Maxflo T impeller (normalized with respect to D/T = 0.35)

At intermediate impeller diameter to tank diameter ratios ($0.25 \leq D/T \leq 0.55$), the just-suspended power requirements are nearly constant, varying by about only twenty-five percent. At large impeller diameter to tank diameter ratios ($D/T \geq 0.55$), the just-suspended power requirements increase dramatically with increasing impeller diameter to tank diameter ratio.

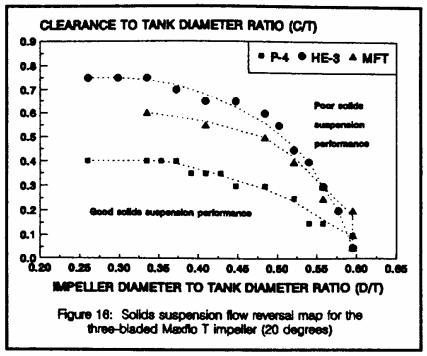

Figure 16: Solids suspension flow reversal map for the three-bladed Maxflo T impeller (20 degrees)

The increase in just-suspended speed, torque, and power at large impeller diameter to tank diameter ratios is due to the change in flow pattern discussed previously (Bakker et al., 1994b). At large impeller diameter to tank diameter ratios and/or high off-bottom clearances, the discharge flow from an axial-flow impeller impinges on the vessel wall rather than the vessel base. This leads to reversed (radially-inward) flow on the vessel base with velocities lower than those that occur when the flow across the vessel base is directed radially-outward. The impeller off-bottom clearance where flow reversal occurs depends on the impeller diameter to tank diameter ratio as shown in Figure 16. The geometries that lead to flow reversal with the Maxflo T are similar to those of the HE-3 at large impeller diameter to tank diameter ratios and intermediate between those of the P-4 and HE-3 at small impeller diameter to tank diameter ratios (the P-4 and HE-3 data has been reported by Myers et al., 1996b).

CONCLUSIONS

The influence of design variables, particularly the number of blades and blade tip angle, on the behavior of the Maxflo T impeller has been characterized. This impeller has an intermediate power number, between those of high-efficiency impellers and pitched-blade turbines. The Maxflo T provides superior performance to that of a pitched-blade turbine and can be applied where high-efficiency impellers encounter critical speed and/or large diameter limitations.

ACKNOWLEDGEMENTS

The assistance of Joseph Duffy, Eric Janz, Aaron Thomas, Mark Reeder, and Jim Nordmeyer with the experiments reported here is gratefully acknowledged.

NOTATION

- C Impeller off-bottom clearance (measured from the lowest point on the impeller), m
- D Impeller diameter, m
- g Acceleration of gravity, m/s^2
- k Just-suspended speed correlating parameter of Equation 7
- M Torque, N·m
- N Agitation speed, s^{-1}
- N_A Aeration number (Q_g/ND^3)
- N_b Number of impeller blades, -
- N_{Fr} Froude number (N^2D/g), -
- N_{js} Just-suspended speed, s^{-1}
- N_p Impeller power number ($P/\rho N^3D^5$), -
- n_p Number of upper axial-flow pumping impellers in a mixed impeller system, -
- N_{Re} Impeller Reynolds number (ND^2/ν), -
- P Impeller power draw, W
- Q_g Volumetric gas flow rate, m^3/s
- S Impeller separation, m
- T Vessel diameter, m
- u_s Adjusted settling velocity ($(\rho_s - \rho_l)u_t/\rho_l$), m/s
- u_t Terminal particle settling velocity in quiescent liquid, m/s
- W Impeller blade width, m
- X Solids loading (solids weight/slurry weight), -
- Z Liquid level, m

Greek Symbols

α Mixed impeller system power split parameter of Equations 3 and 4, -
β Blade tip angle, degrees
ρ Density, kg/m^3
ν Kinematic viscosity, m^2/s

Subscripts

CD-6 refers to the six-bladed, curved-blade disc impeller
D refers to the dispersing impeller of a mixed impeller system
g refers to gassed conditions
HE-3 refers to the three-bladed, high-efficiency HE-3 impeller
l refers to liquid
M refers to a mixed impeller system
MFT refers to the Maxflo T impeller
o refers to ungassed conditions
P refers to the pumping impeller(s) of a mixed impeller system
P-4 refers to the four-bladed, 45° pitched-blade turbine
s refers to solid

REFERENCES

Bakker, A., J. M. Smith, and K. J. Myers, *Chem. Eng.*, 101 (12), 98-104 (1994a).

Bakker, A., J. B. Fasano, and K. J. Myers, *IChemE Symp. Ser.*, 136, 1-8 (1994b).

Buckland, B. C., K. Gbewonyo, D. Jain, K. Glazomitsky, G. Hunt, and S. W. Drew, in *2nd International Conference on Bioreactor Fluid Dynamics*, 1-15 (1988).

Corpstein, R. R., J. B. Fasano, and K. J. Myers, *Chem. Eng.*, 101 (10), 138-144 (1994).

Fasano, J. B., A. Bakker, and W. R. Penney, *Chem. Eng.*, 101 (8), 110-116 (1994).

Gbewonyo, K., D. DiMasi, and B. C. Buckland, in *International Conference on Bioreactor Fluid Dynamics*, 281-299 (1986).

McFarlane, C. M., and A. W. Nienow, *Biotechnol. Prog.*, 11, 601-607 (1995).

Myers, K. J., R. W. Ward, and A. Bakker, submitted to *J. Fluids Eng.* (1996a)

Myers, K. J., A. Bakker, and R. R. Corpstein, submitted to *Can. J. Chem. Eng.* (1996b).

Myers, K. J., J. Fasano, and A. Bakker, *IChemE Symp. Ser.*, 136, 65-72 (1994).

Russell, M. I., Thesis, University of Dayton, Dayton, Ohio, USA (1995).

Willert, C. E., and M. Gharib, *Exp. in Fluids*, 10, 181-193 (1991).